PHYSICAL REVIEW A **86**, 060501(R) (2012)

Observation of the 717-nm electric quadrupole transition in triply charged thorium

A. G. Radnaev,[1,2] C. J. Campbell,[1] and A. Kuzmich[1]
[1]*School of Physics, Georgia Institute of Technology, Atlanta, Georgia 30332-0430, USA*
[2]*KLA-Tencor Corporation, Milpitas, California 95035, USA*
(Received 16 October 2012; published 26 December 2012)

We excite the 717-nm electric quadrupole $6D_{3/2} \leftrightarrow 7S_{1/2}$ transition in a laser-cooled $^{232}Th^{3+}$ ion crystal. The transition frequency and the lifetime of the metastable $7S_{1/2}$ level are measured to be 417 845 964(30) MHz and 0.60(7) s, respectively. We subsequently employ the $7S_{1/2}$ level to drive the ions with nanosecond-long 269-nm laser pulses into the $7P_{1/2}$ level. The latter is connected to the $7S_{1/2}$ electronic level within the ^{229}Th nuclear isomer manifold by the strongest available electron-bridge transition, forming a basis for its laser excitation.

DOI: 10.1103/PhysRevA.86.060501 PACS number(s): 32.10.−f, 07.77.−n, 21.10.−k, 37.10.Rs

State-of-the-art trapped-ion frequency standards utilize narrow optical transitions between valence electron orbitals within a single ion confined in an rf trap. These clocks are currently limited to fractional inaccuracies of $\sim 10^{-17}$ [1–4]. A nuclear transition between two levels of identical electronic quantum numbers in a single ^{229}Th ion could also be used as the basis for a clock [5]. With suitably chosen states in the compound system (nuclear + electronic), all leading-order external-field clock shift mechanisms can be eliminated, leaving only higher-order, significantly smaller shifts. This would relax technical requirements as compared to conventional optical clocks and potentially allow for fractional inaccuracies of $\sim 10^{-19}$ [6].

An important potential application of the ^{229}Th nuclear clock is in the search for temporal variation of fundamental constants, particularly the fine-structure constant α. The most accurate laboratory searches for α variation to date are performed by measuring the ratio of atomic clock frequencies derived from different atomic systems over a long period of time. Because the two different systems have different sensitivities to α variation, the two clock frequencies will differentially shift, changing the frequency ratio. The keys to a sensitive probe are precise frequency measurement of the clock transitions and greatly different sensitivities of the transitions to change in α. In the case of the ^{229}Th nuclear transition, a large enhancement over atomic systems in α-variation sensitivity is predicted to exist due to near-cancellation of the electromagnetic repulsion of the protons and of strong interactions among the nucleons [7,8]. This enhancement, combined with the clock transition's extreme accuracy potential, would lead to an improvement upon the current best measurement of α variation by possibly as many as five orders of magnitude when using state-of-the-art clock technology.

The most recent and precise published measurement of the ^{229}Th isomer energy is 7.8(5) eV [9]. In order to span $\pm 3\sigma$ in the search for this nuclear level, direct optical excitation of the isomer in trapped cold ions may not be a viable method, given available UV sources and the large energy uncertainty. Instead, the electron-bridge process may be utilized, Fig. 1 [10]. In this case, hyperfine-induced mixing of the ground and isomer nuclear manifolds opens up electric dipole transitions between the two. Mixing is expected to be the strongest for the S electronic states, as the electron probability density at the nucleus is highest. For example, considering only the $7S_{1/2}$ and $8S_{1/2}$ electronic orbitals in first-order perturbation theory,

$$\overline{|7S_{1/2}\rangle_e|m\rangle_n} \approx |7S_{1/2}\rangle_e|m\rangle_n + \frac{\langle g|_n\langle 8S_{1/2}|_e H_{\rm int}|7S_{1/2}\rangle_e|m\rangle_n}{E_{(7S_{1/2};m)} - E_{(8S_{1/2};g)}}|8S_{1/2}\rangle_e|g\rangle_n,$$

where the indices e and n indicate electronic and nuclear subspaces, $H_{\rm int}$ is the electron-nucleus interaction Hamiltonian, and $|g\rangle_n = |5/2^+[633]\rangle$, $|m\rangle_n = |3/2^+[631]\rangle$ correspond to the nuclear ground and isomer levels respectively (the nuclear state quantum numbers are in Nilsson classification). The $|8S_{1/2}\rangle_e|g\rangle_n$ admixture couples to the $|7P_{1/2}\rangle_e|g\rangle_n$ level via electric dipole radiation of frequency $(E_{(7S_{1/2};m)} - E_{(7P_{1/2};g)})/\hbar$ (see Fig. 1). This shifts the spectral interrogation region from the challenging 130–200 nm range to the more promising 260–730 nm range.

A search for the nuclear isomer via the electron bridge in laser-cooled $^{229}Th^{3+}$crystals will involve excitation to the $|7P_{1/2}\rangle_e|g\rangle_n$ level, followed by illumination with intense optical radiation which is tunable in the 260–730 nm range. Nuclear transition events will be manifested by interruptions in laser fluorescence on one of the laser cooling transitions. A chain of laser-cooled $^{229}Th^{3+}$ ions will provide near-unity detection efficiency of isomer state population, as well as strong localization for tight focusing of the isomer search light [11]. In this paper, we demonstrate the first important step in this electron-bridge-assisted isomer search by exciting $^{232}Th^{3+}$ ions to the $7P_{1/2}$ level via the three-step process (i) $5F_{5/2} \rightarrow 6D_{3/2}$ excitation at 1088 nm, (ii) $6D_{3/2} \rightarrow 7S_{1/2}$ electric quadrupole excitation at 717 nm, and (iii) $7S_{1/2} \rightarrow 7P_{1/2}$ excitation at 269 nm.

In order to populate the $7S_{1/2}$ level, the $6D_{3/2} \rightarrow 7S_{1/2}$ electric quadrupole transition at 717 nm is utilized. The ^{232}Th isotope is used for this initial work due to its natural abundance and simplified atomic structure, i.e., lack of nuclear spin.

The quadrupole Rabi frequency between states $|i\rangle$ and $|f\rangle$ due to an electric field of amplitude $\mathbf{E}_0$ and wave vector $\mathbf{k}$ is

$$\Omega_Q = \frac{k_\alpha \langle i|Q_{\alpha\beta}|f\rangle (E_0)_\beta}{\hbar}.$$

The electric quadrupole matrix element $\langle i|Q_{\alpha\beta}|f\rangle$ can be obtained using the Wigner-Eckart theorem and the reduced electric quadrupole moment $\langle 6D_{3/2}||Q_{\alpha\beta}||7S_{1/2}\rangle = 7.0631ea_0^2$ [12]. The 717-nm light is created by an external cavity diode laser, where the frequency is stabilized to a transfer cavity as

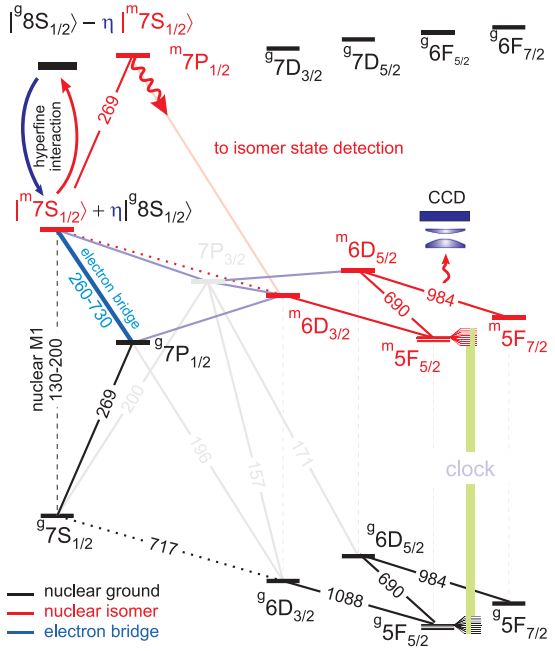

FIG. 1. (Color online) A diagram of electronic energy levels and transitions in $^{229}Th^{3+}$ including both nuclear ground and excited isomeric manifolds. The hyperfine interaction between the nucleus and the valence electron mixes electronic levels of the nuclear ground and isomer manifolds. The mixing is strongest between the $|8S_{1/2}\rangle_e|g\rangle_n$ and $|7S_{1/2}\rangle_e|m\rangle_n$ levels, creating a $|7P_{1/2}\rangle_e|g\rangle_n \rightarrow |7S_{1/2}\rangle_e|m\rangle_n$ electron bridge with effective dipole moment $d_{EB} \approx 2 \times 10^{-5} ea_0$ [13]. This is substantially stronger than the direct nuclear $M1$ transition and also shifts the excitation frequency to a more convenient wavelength range. The superscripts g and m stand for the nuclear ground $|g\rangle_n$ and the isomer $|m\rangle_n$ manifolds, respectively.

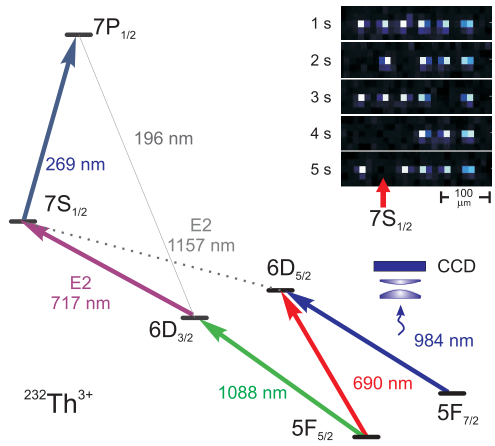

FIG. 2. (Color online) Schematic of atomic levels used in the excitation of the 717-nm electric quadrupole $6D_{3/2} \rightarrow 7S_{1/2}$ and the 269-nm $7S_{1/2} \rightarrow 7P_{1/2}$ transitions. State detection is performed with 984-nm fluorescence measurements. A 5-s-long sequence of images of a $^{232}Th^{3+}$ chain shows ion excitation to the metastable $7S_{1/2}$ level via the 717 nm electric quadrupole transition. In the images, a dark spot typically corresponds to an ion in the metastable $7S_{1/2}$ level, rather than a pollutant ion, inferred from the constant chain structure and observed dynamics when illuminated with the 717-nm field.

described in Ref. [11]. An electro-optical phase modulator, driven by a voltage-controlled oscillator, is used to transfer $\sim$1 mW of optical power to ion resonance with the $+1$ order rf sideband. The laser field is focused to a 110 μm diameter at the ions and corresponds to an electric quadrupole Rabi frequency $\Omega_Q \sim 100$ kHz. This value is sufficient to search the 2 GHz uncertainty region of the previously available indirect frequency measurement of 417 835(2) GHz that employed a gas discharge [14].

The apparatus for creating, trapping, and laser cooling Th^{3+} is described in Ref. [11]. The trap rf frequency is increased to 8 MHz, which allows for operation without the aid of buffer gas. The electric quadrupole transition search protocol (Fig. 2) consists of two main steps: (i) excitation to the metastable $7S_{1/2}$ level and (ii) measurement of its population. For excitation of crystallized ions, the 690-nm repumping field is turned off and the atoms are optically pumped to the ground level with 984-nm light. They are then excited to the $6D_{3/2}$ level with an axial 1088-nm field, corresponding to a $\sim$10-MHz Rabi frequency, and the frequency of the cw 717-nm excitation field is scanned. State detection is accomplished by measuring the population in the metastable $5F_{7/2}$ level, populated with the reintroduction of the 690-nm field. If an ion makes a transition to the $7S_{1/2}$ level, it is no longer resonant with the 984-nm detection field and does not scatter light, as illustrated in Fig. 2. For the search, the interaction time is chosen to be 0.5 s, which is greater than the detection time of 0.1 s, but smaller than the theoretically predicted 0.59 s excited-state lifetime [12].

For the search, the 717-nm laser frequency, spectrally broadened to $\approx$500 MHz, is scanned in 500-MHz steps until the first transition is detected, after which the frequency is recorded. The broadening is achieved by modulating the control voltage of the voltage-controlled oscillator which drives the electro-optical phase modulator. Specifically, a sawtooth wave form with period much shorter than the 0.5 s integration time is added to the dc signal. The sequence is then modified to optimize the excitation rate with a shorter excitation time of 50 ms and with the spectral broadening removed. The 717-nm and 1088-nm fields are alternating with 0.5-μs on-off periods to avoid Stark shifts due to the strong 1088-nm field. The rate of excitation to the $7S_{1/2}$ level is measured as a function of 717-nm field frequency, as shown in Fig. 3. The $6D_{3/2} \rightarrow 7S_{1/2}$ transition frequency in $^{232}Th^{3+}$ is measured to be 417 845 964(30) MHz, as derived from a Lorentzian fit to the data and a corresponding wave-meter frequency measurement. Our measured transition frequency is $\approx$10 GHz higher than that given in Ref. [14]. Estimated light, magnetic, and micromotion shifts are below 1 MHz; therefore the frequency uncertainty of 30 MHz is dominated by the wave-meter (LM-007) inaccuracy. The wave meter is calibrated using a 780-nm laser which is stabilized absolutely to better than 1 MHz via saturated absorption spectroscopy of a rubidium vapor cell. The calibration is also checked against the rubidium $D1$ line at 795 nm and the 690-nm, 984-nm, and 1088-nm transitions in $^{232}Th^{3+}$.

With the ability to efficiently transfer and observe population, this system is used to measure the lifetime of the $7S_{1/2}$ level. The protocol starts with a 50-ms excitation pulse, followed by a variable delay and a 100-ms-long fluorescence detection period. The total period of the sequence is set to 1 s to ensure return of the ions to the ground level. The

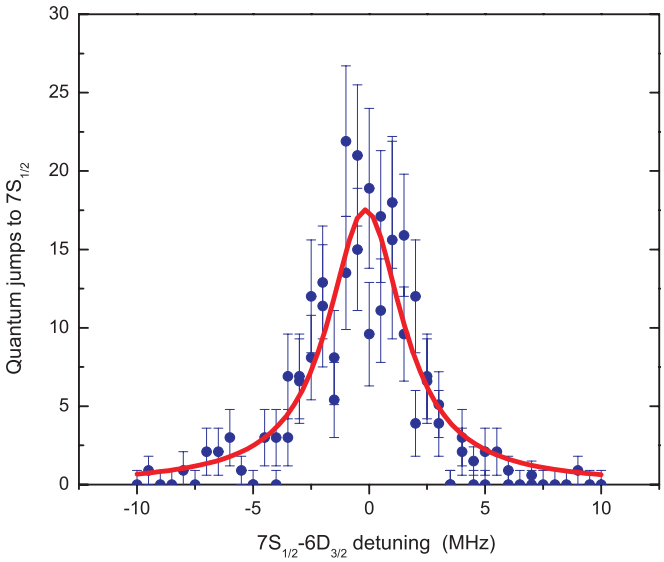

FIG. 3. (Color online) The recorded number of quantum jumps in 300 trials as a function of the 717-nm laser detuning (see text for details).

population of the $7S_{1/2}$ level at various delays is shown in Fig. 4. The exponential fit gives a lifetime of 0.60(7) s, in good agreement with the theoretically predicted value of 0.59 s [12]. A significant systematic error can arise from residual $6D_{3/2} \leftrightarrow 7S_{1/2}$ coupling caused by imperfect attenuation (80 dB) of the 717-nm field after excitation. The residual 717-nm field, with linewidth $\Delta\nu_L \sim 1$ MHz, transfers $7S_{1/2}$ population at a rate $\sim 10^{-8} \times \Omega_Q^2/\Delta\nu_L \sim 10^{-4}$ s^{-1}, corresponding to an $\sim$0.6 s $\times$ [(0.6 s)/(10^4 s)] = 36 μs systematic shift that is much smaller than the statistical error of 0.07 s.

The $|7P_{1/2}\rangle_e|g\rangle_n$ level is the initial state of the strongest electron-bridge transition, $|7P_{1/2}\rangle_e|g\rangle_n \rightarrow |7S_{1/2}\rangle_e|m\rangle_n$. Because the $7S_{1/2}$ level can be populated with the electric quadrupole transition at 717 nm, the 269-nm $7S_{1/2} \rightarrow 7P_{1/2}$

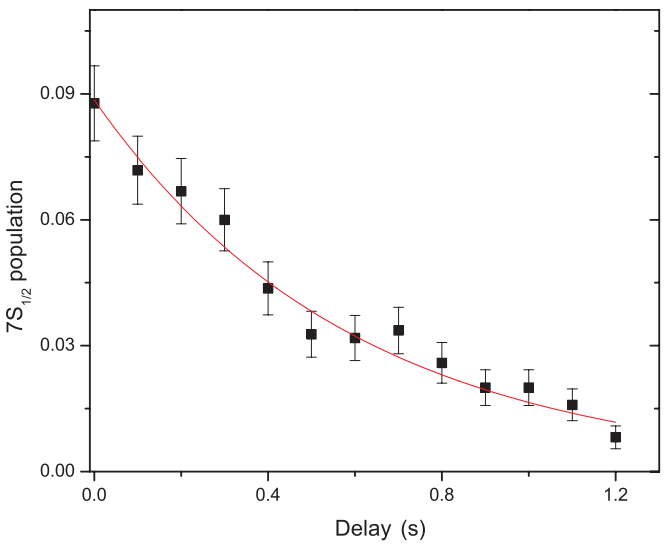

FIG. 4. (Color online) Population of the $7S_{1/2}$ level as a function of the measurement delay. The exponential fit gives a $1/e$ lifetime of 0.60(7) s.

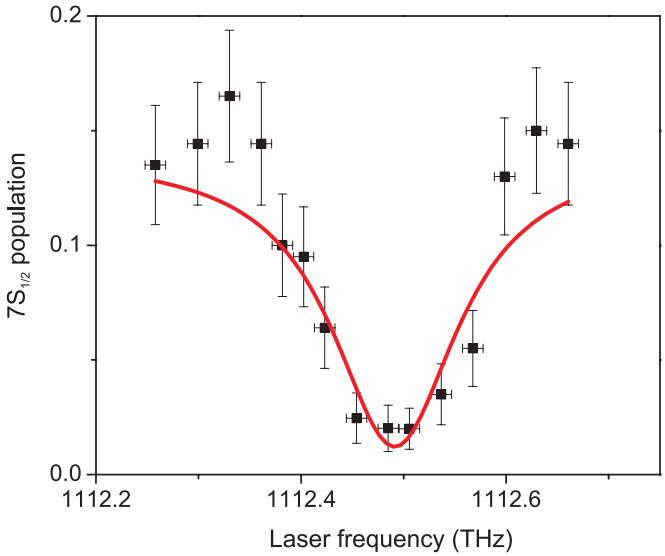

FIG. 5. (Color online) Measured population of the $7S_{1/2}$ level as a function of the 269-nm light frequency. Depopulation of the $7S_{1/2}$ level occurs when the 269-nm laser light is resonant with the $7S_{1/2} \leftrightarrow 7P_{1/2}$ transition.

D_1 transition is a natural route toward population of the $7P_{1/2}$ level.

The laser light for excitation of this transition is obtained by a single-pass doubling of 539-nm light, generated by a home-built optical parametric oscillator (OPO). The OPO is based on a β-barium borate crystal pumped at 10 Hz with 10-ns-long, 355-nm pulses via the third harmonic of a flash-lamp-pumped YAG laser. The Littman configuration of the OPO cavity allows for frequency tuning with a grating. The protocol for $7S_{1/2} \rightarrow 7P_{1/2}$ spectroscopy is based on the sequence described above, with the addition of 269-nm light, as shown in Fig. 2. The 717-nm laser excites ions into the metastable $7S_{1/2}$ level, revealed as dark spots in the ion chain of Fig. 2. When the 269-nm field is resonant with the $7S_{1/2} \rightarrow 7P_{1/2}$ transition, the atoms are strongly excited from the $7S_{1/2}$ metastable level for the duration of the pulse and the short ($\sim$1 ns) lifetime of the $7P_{1/2}$ level ensures rapid decay to the $|6D_{3/2}\rangle$ level. As the frequency of the 269-nm laser is scanned, the metastable state population is measured, as presented in Fig. 5. The high contrast of the dip suggests nearly complete depopulation of the $7S_{1/2}$ level. The average intensity of the 269-nm laser is reduced to about 0.1 mW/cm^2 of cw equivalent to minimize the linewidth of the spectroscopic signal, which is ultimately comparable to the expected linewidth of the 269-nm field. Complete population transfer is observed when the intensity is not reduced for the line narrowing.

With precise control of $7S_{1/2}$ and $7P_{1/2}$ excitation now realized in $^{232}Th^{3+}$, the next step will be to apply the techniques demonstrated here to the ^{229}Th isotope. The transition frequencies between levels in $^{229}Th^{3+}$ are significantly shifted from those of the ^{232}Th isotope due to large relative isotope shifts. The measured isotope shift for the $6D_{3/2}$ level, with respect to the $5F_{5/2}$ ground level, is $-9.856(10)$ GHz [11]. For the $7S_{1/2}$ level, theory predicts an isotope shift coefficient of 146(4) GHz/fm^2 with respect to the $5F_{5/2}$ ground level [15]. Using the radius change $\langle r^2\rangle_{229} - \langle r^2\rangle_{232} = -0.319(33)$ fm^2

based on Refs. [11,16], we obtain a $-37(5)$-GHz expected relative isotope shift for the $6D_{3/2} \rightarrow 7S_{1/2}$ transition. The hyperfine splitting of the $7S_{1/2}$ level in $^{229}Th^{3+}$ is predicted to be 18(1) GHz. The hyperfine structure and relative isotope shift of the $7P_{1/2}$ level is expected to be covered by the $\sim$100 GHz linewidth of the 269-nm excitation field. It is important that this applies to the 269-nm transition within the nuclear isomer manifold. The same field used for excitation to the electron bridge will also serve, once the isomer level is populated, to efficiently and rapidly transfer population from the $|7S_{1/2}\rangle_e|m\rangle_n$ level to the $|6D_{3/2}\rangle_e|m\rangle_n$ level for nuclear state detection.

It should be noted that the $|7P_{1/2}\rangle_e|g\rangle_n$ electron-bridge level can be populated with an alternative scheme—direct excitation from the ground state via the $5F_{5/2} \rightarrow 7P_{1/2}$ two-photon transition at 329 nm. This scheme has the advantage of requiring fewer laser fields; however, the excitation pulses must be of much higher intensity. We have confirmed that Th^{3+} ions maintain a state of crystallization when exposed to high-energy (100 mJ, 5 ns), tightly focused (40-μm-diameter beam) pulses at 355 nm. Because the 329-nm excitation scheme requires light with much less intensity than this, the protocol should be feasible. The two-photon 329-nm scheme is a natural choice when the isomer excitation pulses are shorter than the $|7P_{1/2}\rangle$ excited-state lifetime of $\sim$1 ns and when the pulse repetition rate is less than the $|7S_{1/2}\rangle$ decay rate of $1.7\ s^{-1}$. In this case, a 269-nm repumping field is not necessary. Otherwise, the 717-nm route may be more convenient.

Precise observation of the forbidden 717-nm transition, of which the transition frequency was not previously well known, also demonstrates that the current method of state detection is suitable for an efficient search of the electron-bridge-assisted forbidden nuclear isomer transition in $^{229}Th^{3+}$.

This work was supported by the Office of Naval Research and the National Science Foundation.

[1] T. Rosenband *et al.*, Science **319**, 1808 (2008).
[2] Chr. Tamm, S. Weyers, B. Lipphardt, and E. Peik, Phys. Rev. A **80**, 043403 (2009).
[3] M. Chwalla *et al.*, Phys. Rev. Lett. **102**, 023002 (2009).
[4] C. W. Chou, D. B. Hume, J. C. J. Koelemeij, D. J. Wineland, and T. Rosenband, Phys. Rev. Lett. **104**, 070802 (2010).
[5] E. Peik and Chr. Tamm, Europhys. Lett. **61**, 181 (2003).
[6] C. J. Campbell *et al.*, Phys. Rev. Lett. **108**, 120802 (2012).
[7] V. V. Flambaum, Phys. Rev. Lett. **97**, 092502 (2006).
[8] E. Litvinova, H. Feldmeier, J. Dobaczewski, and V. Flambaum, Phys. Rev. C **79**, 064303 (2009).
[9] B. R. Beck *et al.*, Phys. Rev. Lett. **98**, 142501 (2007); Report No. LLNL-PROC-415170, 2009 (unpublished).
[10] C. J. Campbell *et al.*, Phys. Rev. Lett. **102**, 233004 (2009).
[11] C. J. Campbell, A. G. Radnaev, and A. Kuzmich, Phys. Rev. Lett. **106**, 223001 (2011).
[12] U. I. Safronova, W. R. Johnson, and M. S. Safronova, Phys. Rev. A **74**, 042511 (2006).
[13] S. G. Porsev and V. V. Flambaum, Phys. Rev. A **81**, 032504 (2010).
[14] P. Klinkenberg, Physica B + C **151**, 552 (1988).
[15] J. C. Berengut, V. A. Dzuba, V. V. Flambaum, and S. G. Porsev, Phys. Rev. Lett. **102**, 210801 (2009).
[16] I. Angeli, At. Data Nucl. Data Tables **87**, 185 (2004).